Thermo-phototronic Effect in Double Semiconductor Heterostructures for Highly Sensitive Self-Powered Sensors

Hung Nguyen,* Duy Van Nguyen, Thi Lap Tran, Dzung Viet Dao, Nam-Trung Nguyen, John Bell, and Toan Dinh*

Cite This: *ACS Appl. Electron. Mater.* 2024, 6, 6957−6964

Read Online

| ACCESS | | Metrics & More | | Article Recommendations | | Supporting Information |

ABSTRACT: Understanding the sensing mechanism and the structure−property relationship of self-powered, ultrasensitive photodetectors and temperature sensors is essential for their development. In this study, we report the thermo-phototronic effect observed in double semiconductor heterostructures capable of light harvesting and ultrasensitive temperature sensing. To demonstrate the advances of using the double heterostructure, we conducted a comparative study with a single heterostructure of highly doped n-3C-SiC/p-Si to understand the light harvesting capability and sensing performance. Our results show that the double n-3C-SiC/p-Si heterostructure outperformed the single counterpart in both photovoltage generation and sensitivity, confirming that the structural design significantly impacts the sensing performance of the devices. Under 7.5 mW/cm^2 illumination, the measured voltage in the double structure changed by 21 mV under a 0.2 K temperature gradient, corresponding to an ultrahigh sensitivity of 110 mV/K. This sensitivity is more than 300 times higher than that of 0.3 mV/K observed in the single heterostructure. The underlying physics is attributed to the structural design of the double n-3C-SiC/p-Si heterostructure that controls charge carrier diffusion from the illuminated electrode to the other, resulting in a high photovoltage. These findings demonstrate that using the double n-3C-SiC/p-Si heterostructures can significantly enhance the sensitivity compared with using the single heterostructures, thereby contributing significantly to the development of self-powered photodetectors and temperature sensors.

KEYWORDS: thermo-phototronic, photodetector, temperature sensor, silicon carbide heterostructure, microsensors, temperature gradient, double junction
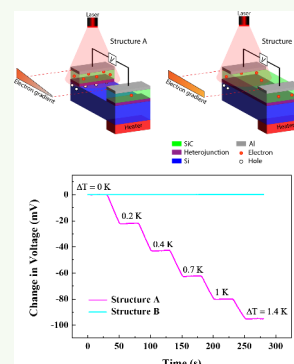
INTRODUCTION

Self-powered sensors represent a significant advancement in sensing technology, offering the potential to operate autonomously without reliance on external power sources.[1] The use of self-powered sensors is crucial in fields where continuous monitoring is essential, such as environmental monitoring, industrial automation, and healthcare.[2−4] The key to the functionality of self-powered sensors lies in their ability to harness ambient energy from the surrounding environment, thereby enabling sustainable and continuous operation. Among the various forms of ambient energy, light and thermal energy emerge as particularly abundant sources, often found together.[5] Therefore, a sensor that can harness both light and thermal energy simultaneously holds great potential to take advantage of the available energy sources.

In recent years, significant progress has been made in the development of sensors capable of capturing both light and thermal energy, enabling efficient energy conversion and power generation.[6−10] Several works have demonstrated self-powered devices using a single heterostructure.[11−14] For example, the InP/ZnO nanorod heterostructure,[11] n-ZnO/p-CuO heterostructure,[14] and P3HT/ZnO nanowire array heterostructure[13] could harvest energy from light to function autonomously as photodetectors. The use of SiC/Si heterostructures has emerged as a promising approach for improving the sensitivity of self-powered sensors.[15−17] These SiC/Si heterostructures offer wide bandgap, strong chemical resistance, and compatibility with silicon-based electronics, making them well-suited for use in harsh environmental conditions.[16,17] Besides, the production of SiC/Si heterostructures also has a big advantage compared to other heterostructures thanks to the low-cost Si wafers.

There were some reports show that highly doped semiconductors have higher conductivity, higher photoresponse, and faster response time compared to the low-doped ones in optoelectronic applications.[18,19] Some reports indicate that highly doped single n-3C-SiC/p-Si heterostructures can generate highly responsive signals due to the combined effects of thermal and photovoltaic interactions.[20,21] The single 3C-SiC/Si heterostructures are typical and have been intensively studied in some reports.[22−24] However, the electrical properties of double heterostructures are significantly larger than those of

single heterostructures, demonstrating the potential of double heterostructures.[25,26] The thermo-phototronic effect, which involves the manipulation of temperature gradients to enhance photovoltaic effects, holds significant potential for further improving the performance of self-powered sensors.[21,27] Despite these advancements, there remain challenges to be addressed to seamlessly integrate both the light harvesting capability and sensing function in a single structure device with high performance.

In this study, we demonstrate the outstanding thermo-phototronic effect in a double semiconductor heterostructure for a self-powered and ultrasensitive sensor. To demonstrate this effect, we fabricate a double heterostructure from a highly doped n-SiC nanofilm grown on a p-Si wafer. By gaining a deeper understanding of the underlying mechanisms and exploring novel device architectures, we aim to explore the potentials of this effect in the highly doped n-SiC/p-Si heterostructures and highlight the crucial impact of structure design on the performance of the devices. Through experimentation and analysis, we have uncovered notable differences between two distinct sensor configurations: double n-3C-SiC/p-Si hetero-structures as structure A and single n-3C-SiC/p-Si hetero-structures as structure B. The single heterostructure is a traditional design used in lateral photovoltaic devices.[28−30] As a conventional design, single heterostructures have been employed in various types of heterostructure devices, including previous works on SiC/Si photodetectors and sensors.[23,24,31,32] The heterojunction in these devices enhances charge carrier separation, resulting in significant open-circuit voltages as demonstrated in previous studies.[25,26] To further enhance the lateral photovoltage, we introduced a new design by properly etching the SiC layer, termed structure A, for photodetecting and temperature sensing and benchmarked it against structure B.

The results show that the structures can harness both light and thermal energy to power itself. Notably, structure A consistently outperformed structure B in terms of voltage variation across changing temperature gradients and light intensities. The voltage change in structure A can reach up to 110 mV/K in response to a temperature gradient, which is very large compared to 0.3 mV/K observed with structure B, 0.8 mV/K with an N-type SnSe:Br single crystal,[33] 0.75 mV/K with Nb-doped SrTiO$_3$,[34] and 1.5 mV/K with the InP/ZnO nanorod heterostructure.[11] The stability of structure A at all temperature gradients also outperformed that of structure B. Furthermore, we observed that increasing the light intensity enhanced the sensitivity of structure A. Consequently, the outstanding sensing properties of the double n-3C-SiC/p-Si heterostructures hold great potential for applications such as temperature sensors or photodetectors, functioning either as a photodetector or as a temperature sensor with a photonic gate.

RESULTS AND DISCUSSION

Mechanisms and Structure Designs. The thermo-phototronic effect in SiC/Si heterostructures is a combination of the thermal and photovoltaic effects, demonstrating the impact of temperature gradient on the photovoltage of devices. When the heterostructures are nonuniformly illuminated, an electron gradient and a lateral photovoltage between the two electrodes are created. Applying a temperature gradient generates more charge carriers between the two electrodes, thus modulating the voltage between them. The thermo-phototronic effect in two structures fabricated from highly

doped n-3C-SiC/p-Si heterostructures is illustrated in Figures 1a and 1b. Figure 1a shows that the SiC film connecting the two
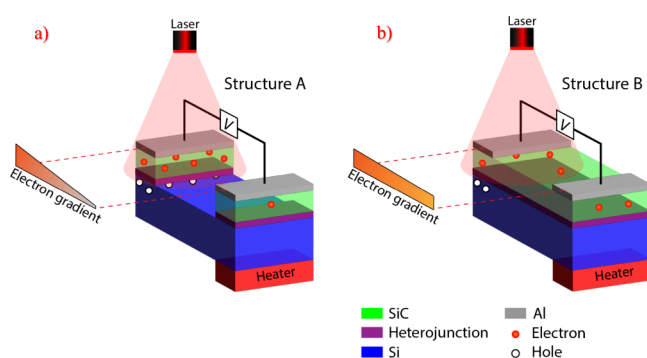
Figure 1. Schematic view and mechanism of the thermo-phototronic effect in (a) structure A (double heterostructures) and (b) structure B (single heterostructure).

electrodes in structure A is removed, while the SiC layer in structure B is not etched, as illustrated in Figure 1b. The unique design of structure A with a double heterostructure significantly improves the electron gradient and photovoltage owing to its ability to prevent the diffusion of charge carriers between the two electrodes.

Figure 2a shows the fabrication process of the devices through photolithography and etching techniques (refer to the Experimental Section for more details). Figure 2b shows an SEM image of the fabricated devices. The gap between the electrodes is approximately 1 mm in both structures A and B. Our study has shown that increasing the electrode spacing can enhance the photovoltage in 3C-SiC/Si heterostructures.[27] The optical images of the devices are shown in Figure S1. Figure 2c shows the I−V characteristics of structures A and B in dark conditions. The I−V characteristic of structure B is linear, indicating an Ohmic contact between SiC and the aluminum electrode. As the voltage in structure A increases, the current is almost zero, confirming its ability to prevent the movement of charge carriers between the two electrodes.

Figure 3a demonstrates the repeatability of the photovoltage of the two structures when they are exposed to laser illumination. The wavelength of the red laser is 635 nm, with light intensities of 3 mW/cm^2. The laser source was alternately turned ON and OFF for 20 s intervals each time. Upon light illumination, the photovoltages exhibited an immediate increase, performing consistent stability. In terms of photo-detection sensitivity, structure A has a sensitivity of 46 mV·cm^2/mW, which is 46 times larger than the 1 mV·cm^2/mW of structure B. The responsiveness and repeatability observed in these signals suggest that light illumination holds promising potential as a stable energy source for self-powered sensors.

The lateral illumination theory in a heterostructure explains how the photovoltage is created, as illustrated in Figures 3c and 3d. The heterojunction plays a key function in generating the voltage. The voltage response is reversible and stable both in darkness and under red laser illumination. With a laser beam wavelength of approximately 635 nm (equivalent to 1.95 eV), photons can pass through the SiC film (which has a bandgap of 2.3 eV) and be captured in the Si layer (with a bandgap of 1.12 eV), thereby generating electron−hole pairs (EHPs) in the Si substrate. The built-in electric field E_0 within the hetero-structure, created by the p-Si and n-SiC layers, drives the
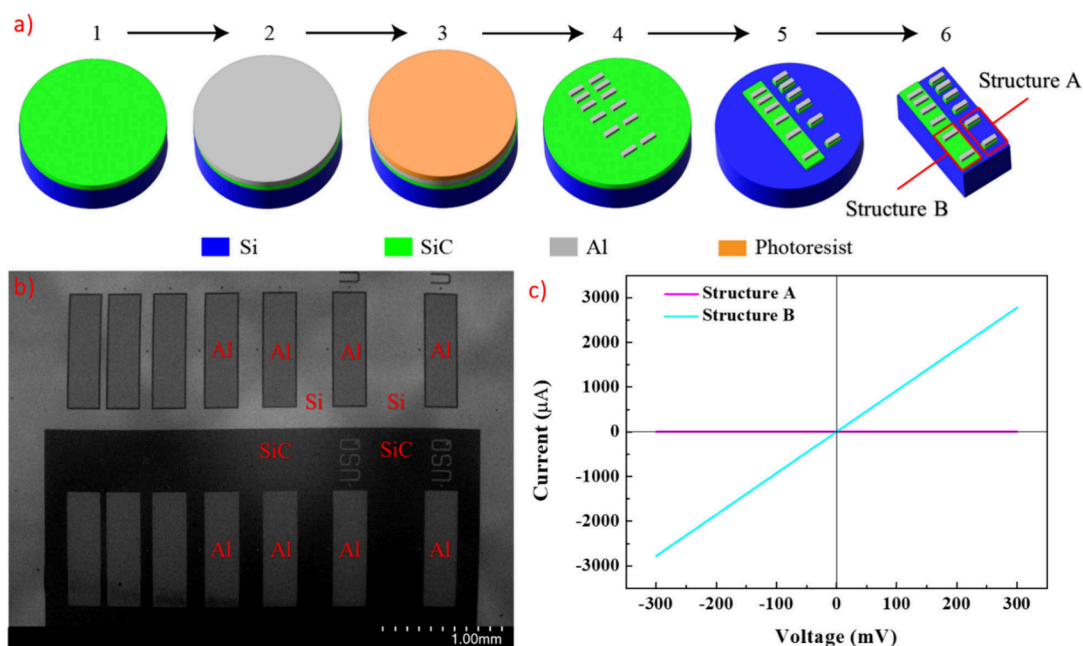
Figure 2. (a) Fabrication process. (b) SEM image of the devices. (c) $I-V$ characteristic of structures A and B in the dark conditions.

electrons toward the SiC layer, while the holes remain in the Si substrate.[20] Consequently, the heterojunction enhances the electron concentration difference between the two electrodes, thus increasing the voltage. The photovoltage in structure A can be evaluated as[35]

$$V = \frac{E_F@L_A - E_F@R_A}{q} = -\frac{k_B T}{q} \ln \frac{e_L}{e_R} \tag{1}$$

where V is the photovoltage, $E_F@L_A$ is the Fermi level of SiC at the electrode L_A, $E_F@R_A$ is the Fermi level of SiC at the electrode R_A, q is the elementary charge, k_B is the Boltzmann constant, T is the temperature, and e_L and e_R are the electron densities at the electrodes L_A and R_A, respectively.

Some former studies investigated the thermo-phototronic effect in single materials. In terms of the mechanism, there are notable differences between our study and former studies that come from the differences in the structure and the sensing effects. While our study investigates the lateral photovoltaic effect in a 3C-SiC/Si heterostructure, previous studies focused on the vertical photovoltaic effect in single materials such as BiFeO$_3$ or an N-type SnSe single crystal. The heterostructure can generate a larger voltage because of the heterojunction. Additionally, the lateral photovoltaic effect requires processing only one side of the materials, whereas the vertical photovoltaic effect in the referenced study requires processing both sides. In terms of device performance, our study showed that the SiC heterostructure has boosted the photovoltage to achieve up to 138 mV at 3 mW/cm^2, corresponding to 46 mV·cm^2/mW, which is significantly higher compared to 2−8 mV·cm^2/mW in BiFeO$_3$ or 1.5−3 mV·cm^2/mW in the N-type SnSe:Br single crystal.[6,33] Therefore, our study has a significant advantage in terms of sensitivity and materials fabrication.

As the laser intensity escalates from 3 to 7.5 mW/cm^2, more photons are absorbed in the Si layer, resulting in additional EHPs generation. As a result, more electrons are propelled toward the SiC layer by the built-in electric field. This increment in the electron density within the illuminated region of the SiC layer intensifies the electron concentration at the electrode L_A,

thereby boosting the photovoltage measurement as shown in Figure 3b. When increasing the light intensity, more EHPs are created but not exactly in proportion to the light intensity. Additionally, the charge carriers pushed to the SiC layer by the built-in electric field might not be exactly proportional either. Therefore, the ratio of increasing voltage is not exactly proportional to the ratio of increasing light intensity as shown in former studies.[20,27] The corresponding results for structure B are shown in Figure S2.

The photovoltage under the same light intensity of structure A is much higher than in structure B. While the SiC layer connecting the two electrodes in structure B was not removed, this allows diffusion of charge carriers from the electrode L_B to the electrode R_B. The diffusion in charge carriers in the structure B can be expressed by Fick's law: $\Gamma_n = -D_n \times \Delta_n/dx$, where Γ_n is electron flow, D_n is the diffusivity coefficient, and Δ_n/dx is the gradient of electrons.[27,35,36] The diffusion of electrons across the SiC layer decreases the difference in charge carriers and Fermi level gap between the electrodes L_B and R_B of structure B as shown in Figures 3d and 3f. While the SiC bridge connecting the two electrodes in structure A was removed, there is no diffusion along the SiC layer from the electrode L_A to the electrode R_A as shown in Figures 3c and 3e. Therefore, the photovoltage of structure A is significantly higher than that of structure B under the same illumination intensity.

Figure 4a shows the voltage response of structures A and B under laser illumination with intensity of 3 mW/cm^2. The temperature gradient was stabilized for 30 s at 0 K, followed by incremental increases and stabilization at 0.2, 0.4, 0.7, 1, and 1.4 K for an additional 30 s at every temperature. These temperature gradients were calculated by subtracting the temperature of the hotter electrode from the temperature of the colder electrode (see Table S1 for more details). The graphs in Figure 4a show that the voltage in structure A steadily drops as the temperature gradient increases, while the change in voltage of structure B is negligible compared to structure A. The photovoltages drop by 22, 43, 62.5, 80, and 95 mV for temperature gradients of 0.2, 0.4, 0.7, 1, and 1.4 K, respectively. By creating the temperature
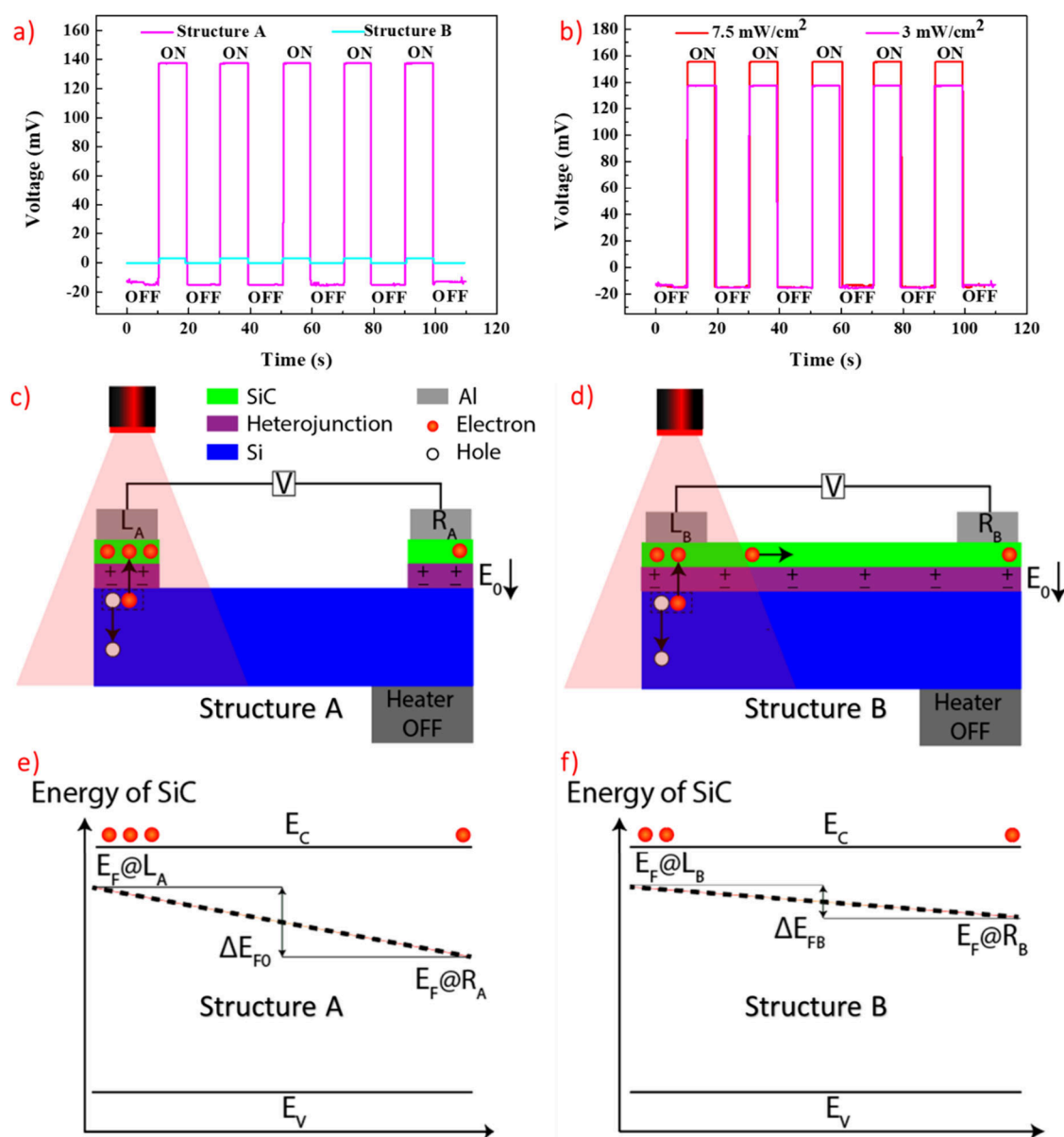
Figure 3. (a) Voltage response of structures A and B under 3 mW/cm^2 illumination. (b) Voltage response of structure A under 3 and 7.5 mW/cm^2 illumination. (c) Experimental setup and physical interactions in structure A. (d) Experimental setup and physical interactions in structure B. (e) Band structure of structure A under illumination. (f) Band structure of structure B under illumination.

gradient by heating the electrode R_A, the temperature in the device also increases (see Table S1 for more details of the temperature between electrodes and respective temperature gradient). Increasing the temperature along the device has been proven to generate more EHPs in the Si layer;[17] the generated electrons are then driven to the n-SiC layer by the electric field E_0. The newly supplied electrons decrease the electron gradient and Fermi level difference between the electrodes L_A and R_A of structure A, as shown in Figures 4c and 4d, which decreases the photovoltage when the temperature is increased. These results have also been confirmed under heating and cooling conditions, where the voltage increases during heating and decreases during cooling, as shown in Figure S3 and former studies.[11,33]

The maximum change observed for structure B is 0.16 mV at a 1.4 K temperature gradient, and this change exhibits instability at each temperature level, as illustrated in Figure S4. Consequently, regarding both stability and resolution across different temperature gradients, structure A shows significant

superiority over structure B for temperature sensing applications.

To further understand the thermo-phototronic behavior of structure A, Figure 4b compares the voltage response of structure A under two laser intensities: 3 and 7.5 mW/cm^2. It is observed that the drop in voltage for 7.5 mW/cm^2 is higher than for 3 mW/cm^2. Since higher light intensity leads to a higher voltage in structure A, as shown in Figure 3b, the electron gradient between the electrodes L_A and R_A of structure A under 7.5 mW/cm^2 illumination is larger than under 3 mW/cm^2 illumination.

When heating the electrode R_A to increase the temperature gradient, the thermally generated electrons decrease the gradient of electrode and Fermi levels between the electrodes L_A and R_A as shown in Figures 4c and 4d. Because the electron gradient for 7.5 mW/cm^2 illumination is higher than that for 3 mW/cm^2, the drop in voltage for 7.5 mW/cm^2 is also higher. See Figure S5 for more details.
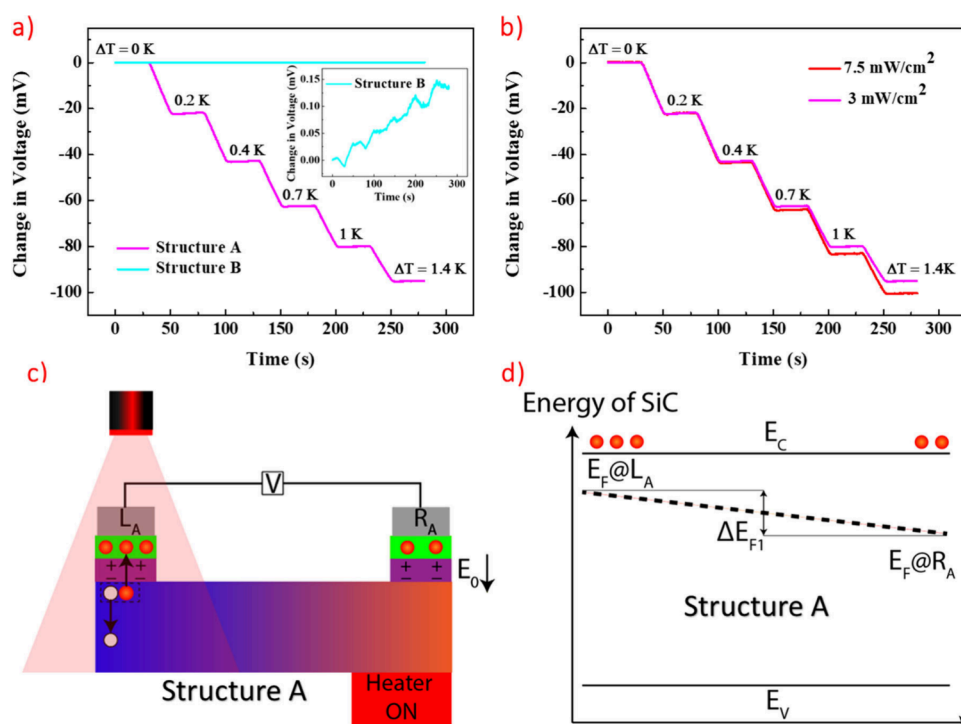
Figure 4. (a) Impact of the temperature gradient on the photovoltage of the two structures A and B when illuminating the left electrode and heating the right electrode. (b) Impact of the temperature gradient on the photovoltage when heating electrode R_A and illuminating electrode L_A of structure A under different light intensities. (c) Experimental setup of structure A under illumination and temperature gradient. (d) Band structure of structure A under illumination and temperature gradient.
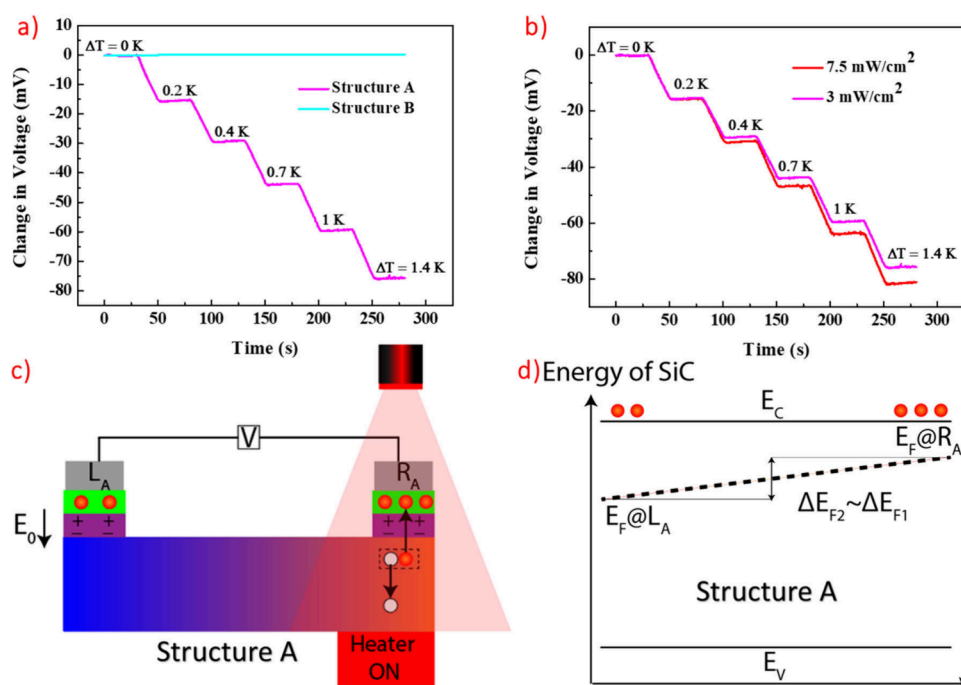
Figure 5. (a) Impact of the temperature gradient on the photovoltage of the two structures A and B when illuminating and heating the right electrode. (b) Impact of the temperature gradient on the photovoltage when heating electrode R_A and illuminating electrode R_A of the structure A under different light intensities. (c) Experimental setup of structure A under illumination and temperature gradient. (d) Band structure of structure A under illumination and temperature gradient.

To further explore the impact of increasing the temperature gradient through heating on structures A and B, we adjusted the illumination position to the right electrode while simultaneously heating it, as depicted in Figure 5.

Figure 5a shows the voltage responses of structures A and B under a 635 nm laser beam under 3 mW/cm² illumination. structure A demonstrates a substantially larger voltage variation compared to structure B when the temperature gradient

between the measured electrodes gradually increased from 0 to 1.4 K, thus affirming the advantage of structure A over structure B regardless of the illuminating position. For details, the maximum sensitivity of structure A is 79 mV/K, outperforming the 0.3 mV/K of structure B. The maximum change in voltage for structure A is 76 mV, much higher than the 0.22 mV for structure B. The change in voltage of structure A is very large compared to the 0.3 mV/K observed with structure B, 0.8 mV/K with N-type SnSe:Br single crystal,[33] 0.75 mV/K with Nb-doped SrTiO$_3$,[34] and 1.5 mV/K with InP/ZnO nanorod heterostructure[11] (see Table S2 for more details). These findings also evidenced that escalating the temperature gradient raises the temperature throughout structure A, consequently leading to an increase in thermally generated electrons at the two electrodes of structure A. The newly generated electrons contribute to a reduction in the electron gradient and the Fermi level difference between the two electrodes, as illustrated in Figures 5c and 5d. Additionally, the voltage decreases when illuminating and heating electrode R_A simultaneously, further indicating that the measured voltage is influenced by the temperature across structure A.

Figure 5b demonstrates trends similar to those in Figure 4b when the light intensity is increased from 3 to 7.5 mW/cm^2. The voltages gradually decrease with increasing temperature gradient due to heating one electrode for both light intensities. Moreover, the voltage drop is higher under 7.5 mW/cm^2 illumination compared to 3 mW/cm^2. This is attributed to the higher electron gradient for 7.5 mW/cm^2 illumination, resulting in a greater impact from thermally generated electrons on the voltage drop. See Figure S6 for more details.

The double highly doped n-3C-SiC/p-Si heterostructure is also more independent of the illumination position compared with the single highly doped n-3C-SiC/p-Si heterostructure. In this study, the change in voltage of structure A is quite similar when changing the illumination position. For the single highly doped n-3C-SiC/p-Si heterostructure like structure B, our previous study showed that the single heterostructure is more dependent on the illumination position. Specifically, when one electrode was illuminated and the other was heated, the voltage increased. Conversely, when illuminating and heating the same electrode, the voltage decreased.[20]

CONCLUSION

In conclusion, we have demonstrated the thermo-phototronic effect in both single and double semiconductor heterostructures using highly doped n-SiC deposited on p-Si. Our investigation highlights the significant impact of structural design on the performance of self-powered sensors that harvest light for ultrasensitive temperature sensing. Through experimentation and analysis, we have revealed that the double heterostructure consistently outperformed the single heterostructure in change of voltage across changing temperature gradients and light intensities. The change in voltage of the double n-3C-SiC/Si heterostructure can be up to 110 mV/K, which is more than 300 times larger than that of the single n-3C-SiC/Si heterostructure. The stability of the double heterostructure at each temperature gradient was also much higher compared with the single heterostructure. Additionally, increasing the light intensity also increased the sensitivity of the double heterostructure. Therefore, the double n-3C-SiC/Si heterostructure holds great potential for temperature sensing and photodetection. These findings have the potential to open new avenues for innovation in sensing technology, confirming the importance of structure

design on the working performance of self-powered temperature sensors and visible light photodetectors toward commercialization.

EXPERIMENTAL SECTION

The SiC/Si heterostructure was fabricated by a photolithography process with the following steps: Start with a commercial p-Si wafer that is 675 μm thick and 150 mm in diameter. A 98 nm highly doped n-SiC layer was grown from the p-Si wafer; the doping concentration in the n-SiC layer is about 10^{19} cm^{-3} (1). The SiC/Si heterostructure was sputtered with a layer of aluminum using a Surrey NanoSystems Gamma 1000C confocal magnetron sputterer (2). Then the heterostructure was covered by a photoresist layer (3). The Al was then etched to create suitable shapes of electrodes for testing (4). The SiC layer was etched to create desired structures (5). Finally, the wafer was diced into smaller devices for testing (6). Since the thickness of the SiC layer is hundreds of times smaller compared to the Si substrate, the specific heat capacity and thermal resistance of the SiC/Si heterostructures are similar to those of Si.[37]

The structure of the SiC layer and electrodes was observed by using a scanning electron microscope (SEM). Then the $I-V$ curve of the device was tested to determine whether the device is ready for characterization. To generate a photovoltage in the n-3C-SiC/p-Si heterostructures, we focused a laser beam with a 635 nm wavelength on top of the one electrode. The laser beam power levels are approximately 1 and 2.5 mW, while the illumination area was fixed at 0.33 cm^2, resulting in light intensities of 3 and 7.5 mW/cm^2, respectively. To raise the temperature gradient in the device, a Linkam HFS600E-PB4 hot plate was placed under the end that has one electrode, while the end with the other electrode was cooled by ambient temperature, creating a temperature gradient across the tested structures. The Linkam HFS600E-PB4 device can adjust the temperature with a precision of 0.1 °C. The electrical characterization was conducted by using a Keithley 2450 source meter.

ASSOCIATED CONTENT

Ⓢ Supporting Information

The Supporting Information is available free of charge at https://pubs.acs.org/doi/10.1021/acsaelm.4c01287.

> Temperature gradient with the respective temperature at electrodes (Table S1); comparison of sensitivity of different materials (Table S2); optical image of the devices (Figure S1); voltage response of structures B under different light intensities (Figure S2); change in photovoltage under heating and cooling conditions (Figure S3); change in voltage of structure B under heating and 3 mW/cm^2 illumination (Figure S4); voltage response while illuminating one electrode and heating the other electrode (Figure S5); voltage response while illuminating and heating the same electrode (Figure S6) (PDF)

AUTHOR INFORMATION

Corresponding Authors

Hung Nguyen − *School of Engineering and Centre for Future Materials, University of Southern Queensland, Toowoomba, Queensland 4350, Australia;* Ⓞ orcid.org/0000-0001-9887-3691; Email: hung.nguyen@usq.edu.au

Toan Dinh − *School of Engineering and Centre for Future Materials, University of Southern Queensland, Toowoomba, Queensland 4350, Australia;* Email: toan.dinh@usq.edu.au

Authors

Duy Van Nguyen − *School of Engineering and Centre for Future Materials, University of Southern Queensland, Toowoomba,*

Queensland 4350, Australia; ⊙ orcid.org/0000-0002-3420-2378

Thi Lap Tran − *School of Engineering and Centre for Future Materials, University of Southern Queensland, Toowoomba, Queensland 4350, Australia*

Dzung Viet Dao − *Queensland Micro- and Nanotechnology Centre, Griffith University, Nathan, Queensland 4111, Australia;* ⊙ orcid.org/0000-0002-6348-0879

Nam-Trung Nguyen − *Queensland Micro- and Nanotechnology Centre, Griffith University, Nathan, Queensland 4111, Australia*

John Bell − *Centre for Future Materials, University of Southern Queensland, Toowoomba, Queensland 4350, Australia*

Complete contact information is available at:
https://pubs.acs.org/10.1021/acsaelm.4c01287

Notes
The authors declare no competing financial interest.

■ REFERENCES

(1) Jin, L.; Tao, J.; Bao, R.; Sun, L.; Pan, C. Self-powered real-time movement monitoring sensor using triboelectric nanogenerator technology. *Sci. Rep.* **2017**, *7* (1), No. 10521.

(2) Park, S.; Heo, S. W.; Lee, W.; Inoue, D.; Jiang, Z.; Yu, K.; Jinno, H.; Hashizume, D.; Sekino, M.; Yokota, T.; Fukuda, K.; Tajima, K.; Someya, T. Self-powered Ultra-flexible Electronics via Nano-grating-patterned Organic Photovoltaics. *Nature* **2018**, *561* (7724), 516−521.

(3) Wang, S.; Lin, L.; Wang, Z. L. Triboelectric Nanogenerators as Self-powered Active Sensors. *Nano Energy* **2015**, *11*, 436−462.

(4) Fuh, Y.-K.; Chen, P.-C.; Huang, Z.-M.; Ho, H.-C. Self-Powered Sensing Elements Based on Direct-Write, Highly Flexible Piezoelectric Polymeric Nano/Microfibers. *Nano Energy* **2015**, *11*, 671−677.

(5) Zhang, Q.; Sun, Y.; Xu, W.; Zhu, D. Organic Thermoelectric Materials: Emerging Green energy Materials Converting Heat to Electricity Directly and Efficiently. *Adv. Mater.* **2014**, *26* (40), 6829−6851.

(6) Qi, J.; Ma, N.; Ma, X.; Adelung, R.; Yang, Y. Enhanced Photocurrent in BiFeO3Materials by Coupling Temperature and Thermo-Phototronic Effects for Self-Powered Ultraviolet Photodetector System. *ACS Appl. Mater. Interfaces* **2018**, *10* (16), 13712−13719.

(7) Gao, T.; Ji, Y.; Yang, Y. Thermo-Phototronic-Effect-Enhanced Photodetectors Based on Porous ZnO Materials. *Adv. Electron. Mater.* **2019**, *5* (12), No. 1900776.

(8) Zou, Z.; Zhao, Z.; Zhang, Z.; Tian, W.; Yang, C.; Jin, X.; Zhang, K. Room-temperature optoelectronic gas sensor based on core−shell g-C3N4@ WO3 heterocomposites for efficient ammonia detection. *Anal. Chem.* **2023**, *95* (3), 2110−2118.

(9) Liu, K.; Tian, W.; Hui, B.; Zhang, K.; Xia, Y. Alginate Fiber Anchored Conductive Coordination Frameworks for Ultrastable Light-gas dual Sensors with Synergistic Effect. *Materials Science and Engineering: R: Reports* **2024**, *160*, No. 100827.

(10) Du, X.; Tian, W.; Zhang, Z.; Hui, B.; Pan, J.; Sun, J.; Zhang, K. Defect Promoted Photothermoelectric Effect in Densely Aligned ZnO Nanorod Arrays for Self-Powered Position-Sensitive Photodetection. *Journal of Materiomics* **2022**, *8* (3), 693−701.

(11) Zhang, K.; Yang, Y. Thermo-Phototronic Effect Enhanced InP/ZnO Nanorod Heterojunction Solar Cells for Self-Powered Wearable Electronics. *Adv. Funct. Mater.* **2017**, *27* (38), No. 1703331.

(12) Zhang, X.; Liu, B.; Yang, W.; Jia, W.; Li, J.; Jiang, C.; Jiang, X. 3D-Branched Hierarchical 3C-SiC/ZnO Heterostructures for High-Performance Photodetectors. *Nanoscale* **2016**, *8* (40), 17573−17580.

(13) Ouyang, B.; Zhang, K.; Yang, Y. Self-Powered UV Photodetector Array Based on P3HT/ZnO Nanowire Array Heterojunction. *Advanced Materials Technologies* **2017**, *2* (12), No. 1700208.

(14) Li, Q.; Meng, J.; Huang, J.; Li, Z. Plasmon-Induced Pyro-Phototronic Effect Enhancement in Self-Powered UV−Vis Detection with a ZnO/CuO p−n Junction Device. *Adv. Funct. Mater.* **2022**, *32* (7), No. 2108903.

(15) Foisal, A. R. M.; Dinh, T.; Nguyen, V. T.; Tanner, P.; Phan, H.-P.; Nguyen, T.-K.; Haylock, B.; Streed, E. W.; Lobino, M.; Dao, D. V. Self-Powered Broadband (UV-NIR) Photodetector Dased on 3C-SiC/Si Heterojunction. *IEEE Trans. Electron Devices* **2019**, *66* (4), 1804−1809.

(16) Nguyen, T.; Van Nguyen, D.; Nguyen, H.; Tong, B.; Tran, C.-D.; Takahashi, H.; Nguyen, N.-T.; Dao, D. V.; Dinh, T. Light Harvesting Self-Powered Strain Sensor using 3C-SiC/Si Heterostructure. *IEEE Sensors* **2022**, 1−4.

(17) Nguyen, T.; Dinh, T.; Bell, J.; Dau, V. T.; Nguyen, N.-T.; Dao, D. V. Light-Harvesting Self-Powered Monolithic-Structure Temperature Sensing Based on 3C-SiC/Si Heterostructure. *ACS Appl. Mater. Interfaces* **2022**, *14* (19), 22593−22600.

(18) Yu, H.; Gao, C.; Zou, J.; Yang, W.; Xie, Q. Simulation Study on the Effect of Doping Concentrations on the Photodetection Properties of Mg2Si/Si Heterojunction Photodetector. *Photonics* **2021**, *8*, 509.

(19) Ganesh, V.; AlAbdulaal, T. Role of Mo-doping Concentration on In2S3 Thin Film for Photodetecting Application by Nebulizer Spray Pyrolysis Method. *Appl. Phys. A: Mater. Sci. Process.* **2023**, *129* (6), 427.

(20) Nguyen, H.; Nguyen, T.; Nguyen, D. V.; Phan, H.-P.; Nguyen, T. K.; Dao, D. V.; Nguyen, N.-T.; Bell, J.; Dinh, T. Enhanced Photovoltaic Effect in n-3C-SiC/p-Si Heterostructure Using a Temperature Gradient for Microsensors. *ACS Appl. Mater. Interfaces* **2023**, *15* (32), 38930−38937.

(21) Nguyen, H.; Nguyen, T.; Van Nguyen, D.; Phan, H.-P.; Nguyen, N.-T.; Dao, D.; Bell, J.; Dinh, T.; et al. Thermo-Phototronic Effect for Self-Powered Photodetector Using n-3C-SiC/p-Si Heterostructure. *IEEE Sensors* **2024**, *124*, 1−4.

(22) Nguyen, T.-H.; Vu, T.-H.; Pham, T. A.; Ninh, D. G.; Nguyen, C. T.; Nguyen, H.-Q.; Tong, B.; Tran, D. D.H.; Streed, E. W.; Dau, V. T.; Nguyen, N.-T.; Dao, D. V. Enhanced lateral photovoltaic effect in 3C-SiC/Si heterojunction under external electric field. *Sensors and Actuators A: Physical* **2023**, *363*, No. 114746.

(23) Foisal, A. R. M.; Nguyen, T.; Dinh, T.; Nguyen, T. K.; Tanner, P.; Streed, E. W.; Dao, D. V. 3C-SiC/Si Heterostructure: An Excellent Platform for Position-Sensitive Detectors Based on Photovoltaic Effect. *ACS Appl. Mater. Interfaces* **2019**, *11* (43), 40980−40987.

(24) Nguyen, T.; Dinh, T.; Foisal, A. R. M.; Phan, H.-P.; Nguyen, T.-K.; Nguyen, N.-T.; Dao, D. V. Giant Piezoresistive Effect by Optoelectronic Coupling in a Heterojunction. *Nat. Commun.* **2019**, *10* (1), 1−8.

(25) Meng, Q.; Lin, Q.; Jing, W.; Mao, Q.; Zhao, L.; Fang, X.; Dong, T.; Jiang, Z. Characterization of the Electrical Properties of a Double Heterostructure GaN/AlGaN Epitaxial Layer with an AlGaN Interlayer. *J. Electron. Mater.* **2021**, *50*, 2521−2529.

(26) Foisal, A. R. M.; Qamar, A.; Nguyen, T.; Dinh, T.; Phan, H. P.; Nguyen, H.; Duran, P. G.; Streed, E. W.; Dao, D. V. Ultra-sensitive Self-Powered Position-sensitive Detector Based on Horizontally-aligned Double 3C-SiC/Si Heterostructures. *Nano Energy* **2021**, *79*, No. 105494.

(27) Nguyen, H.; Nguyen, D. V.; Tran, T. L.; Song, P.; Hong, M.; Dao, D. V.; Nguyen, N.-T.; Bell, J.; Dinh, T. Tunable Thermo-phototronic Effect in Unintentionally Doped n-3C−SiC/p-Si Heterostructure. *Appl. Phys. Lett.* **2024**, *124* (15), 152104.

(28) Tang, Y.; Jin, P.; Wang, Y.; Li, D.; Chen, Y.; Ran, P.; Fan, W.; Liang, K.; Ren, H.; Xu, X.; et al. Enabling Low-drift Flexible Perovskite Photodetectors by Electrical Modulation for Wearable Health Monitoring and Weak Light Imaging. *Nat. Commun.* **2023**, *14* (1), 4961.

(29) Zhang, J.; Meng, K.; Ni, G. Enhanced Lateral Photovoltaic Effects in n-Si/SiO2/PEDOT: PSS Structures. *Polymers* **2022**, *14* (7), 1429.

(30) Yu, C.; Wang, H. Large Lateral Photovoltaic Effect in Metal-(Oxide-) Semiconductor Structures. *Sensors* **2010**, *10* (11), 10155−10180.

(31) Dinh, T.; Nguyen, T.; Foisal, A.; Phan, H.-P.; Nguyen, T.-K.; Nguyen, N.-T.; Dao, D. Optothermotronic Effect as an Ultrasensitive Thermal Sensing Technology for Solid-State Electronics. *Science Advances* **2020**, *6* (22), 2671.

(32) Tran, D.H.D.; Nguyen, T.-H.; Nguyen, C. T.; Streed, E. W.; Nguyen, N.-T.; Dau, V. T.; Dao, D. V. Effect of Mechanical Strain on Lateral Photovoltaic Effect in n-3C-SiC/n-Si Heterojunction: Toward Mechanical Strain Sensors Capable of Photoenergy Harvesting. *Nano Energy* **2024**, *128*, No. 109844.

(33) Yang, L.; Wu, L.; Su, L.; Xu, L.; Zhao, L.-D.; Yang, Y. Enhanced Photodetector at Low-Temperature via Thermo-Phototronic Effect in N-type SnSe: Br Single Crystal. *Nano Energy* **2023**, *107*, No. 108140.

(34) Wu, L.; Ji, Y.; Ouyang, B.; Li, Z.; Yang, Y. Self-Powered Light-Temperature Dual-Parameter Sensor Using Nb-Doped SrTiO3Materials Via Thermo-Phototronic Effect. *Adv. Funct. Mater.* **2021**, *31* (17), No. 2010439.

(35) Kasap, S. *Principles of Electronic Materials and Devices*, 4th ed.; 2018.

(36) Sze, S. M.; Li, Y.; Ng, K. K. *Physics of Semiconductor Devices*; John Wiley & Sons: 2006.

(37) Kukushkin, S.; Markov, L.; Osipov, A.; Svyatets, G.; Chernyakov, A.; Pavlov, S. Thermal Conductivity of Hybrid SiC/Si Substrates for the Growth of LED Heterostructures. *Technical Physics Letters* **2023**, *49* (S4), S327−S329.